We are IntechOpen,
the world's leading publisher of
Open Access books
Built by scientists, for scientists

6,900
Open access books available

186,000
International authors and editors

200M
Downloads

154
Countries delivered to

Our authors are among the

TOP 1%
most cited scientists

12.2%
Contributors from top 500 universities

CLARIVATE ANALYTICS
BOOK CITATION INDEX
INDEXED

WEB OF SCIENCE™

Selection of our books indexed in the Book Citation Index
in Web of Science™ Core Collection (BKCI)

Interested in publishing with us?
Contact book.department@intechopen.com

Numbers displayed above are based on latest data collected.
For more information visit www.intechopen.com

Introduction to Synthetic Aperture Sonar

Roy Edgar Hansen
Norwegian Defence Research Establishment
Norway

1. Introduction

SONAR is an acronym for **SO**und **N**avigation **A**nd **R**anging. The basic principle of sonar is to use sound to detect or locate objects, typically in the ocean. Sonar technology is similar to other technologies such as: RADAR = **RA**dio **D**etection **A**nd **R**anging; ultrasound, which typically is used with higher frequencies in medical applications; and seismic processing, which typically uses lower frequencies in the sediments. There are many good books that cover the topic of sonar (Burdic, 1984; Lurton, 2010; Urick, 1983). There are also a large number of books that cover the theory of underwater acoustics more thoroughly (Brekhovskikh & Lysanov, 1982; Medwin & Clay, 1998).

The principle of Synthetic aperture sonar (SAS) is to combine successive pings coherently along a known track in order to increase the azimuth (along-track) resolution. A typical data collection geometry is illustrated in Fig. 1. SAS has the potential to produce high resolution images down to centimeter resolution up to hundreds of meters range. This makes SAS a suitable technique for imaging of the seafloor for applications such as search for small objects, imaging of wrecks, underwater archaeology and pipeline inspection.

SAS has a very close resemblance with synthetic aperture radar (SAR). While SAS technology is maturing fast, it is still relatively new compared to SAR. There is a large amount of SAR literature (Carrara et al., 1995; Cumming & Wong, 2005; Curlander & McDonough, 1991; Franceschetti & Lanari, 1999; Jakowatz et al., 1996; Massonnet & Souyris, 2008).

This chapter gives an updated introduction to SAS. The intended reader is familiar with sonar but not SAS. The only difference between traditional sonar and synthetic aperture is
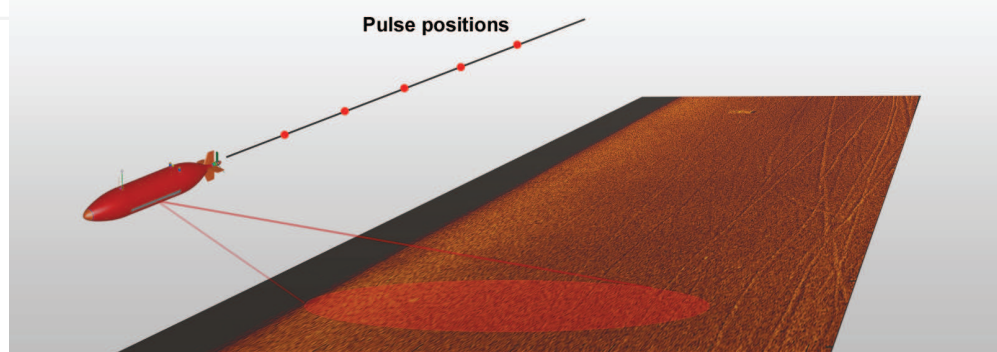

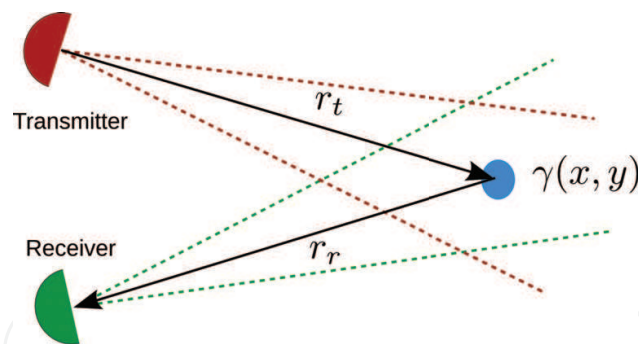Fig. 1. Data acquisition geometry for synthetic aperture sonar.

Fig. 2. Basic imaging geometry.

the construction of the aperture (or array). We start by giving a review of sonar imaging and describe the backprojection method. Then, we derive the angular resolution. We describe the multi-element receiver concept and calculate the area coverage rate for SAS. We explain the frequency dependence in SAS, and discuss some of the choices and trade-offs in SAS design. We list some of the specific challenges in SAS, and suggest possible solutions. We give an overview of the signal processing involved in a SAS processor, and we discuss properties of SAS images. Finally, we show numerous examples of SAS images from a particular system, the HISAS 1030 interferometric SAS.

2. Sonar Imaging

Assume a transmitter that insonifies a scene with acoustic reflecting material represented by a reflectivity function $\gamma(x, y)$. A part of the scattered acoustic field is recorded by one or more receiver hydrophones. This is illustrated in Fig. 2. Sonar imaging is the *inverse problem*, namely to estimate the reflectivity function from the received data from one or more transmitted pulses.

Sonar imaging can be separated into range processing of the data and angular processing (beamforming) of the data. *Beamforming* is defined as the method or processing algorithm that focuses the signal from several receivers in a particular direction. Beamforming can be applied to all types of multi-receiver sonars: active, passive, towed array, bistatic, multistatic, and synthetic aperture. Sonar beamforming is well covered in (Burdic, 1984; Johnson & Dudgeon, 1993; Nielsen, 1991).

Range processing is signal processing applied to each time series individually. The processing is a function of transmit waveform. There are several types of signals that are used as transmit waveforms. Classical sonar often uses gated continuous-wave (CW) pulses, sometimes referred to as pings. Modern sonar, and virtually all SAS systems, use phase coded transmit signals where the signal bandwidth is determined by the phase coding (or frequency spread of the signal modulation). The reason to use phase coded waveforms is to increase the transmit signal energy while maintaining large signal bandwidth. The range processing done on phase coded signals are referred to as *pulse compression* or *matched filtering*. This is covered in a number of excellent books such as (Franceschetti & Lanari, 1999; Levanon, 1988).

2.1 Imaging by backprojection

The simplest and most intuitive type of beamforming is time-domain beamforming by *backprojection*. This is done by back propagating the received signal via each pixel in the scene to be imaged and into the transmitter. This is illustrated in Fig. 3. Backprojection is also known as Delay-And-Sum (DAS) (Johnson & Dudgeon, 1993, pages 117-119). Functionally,
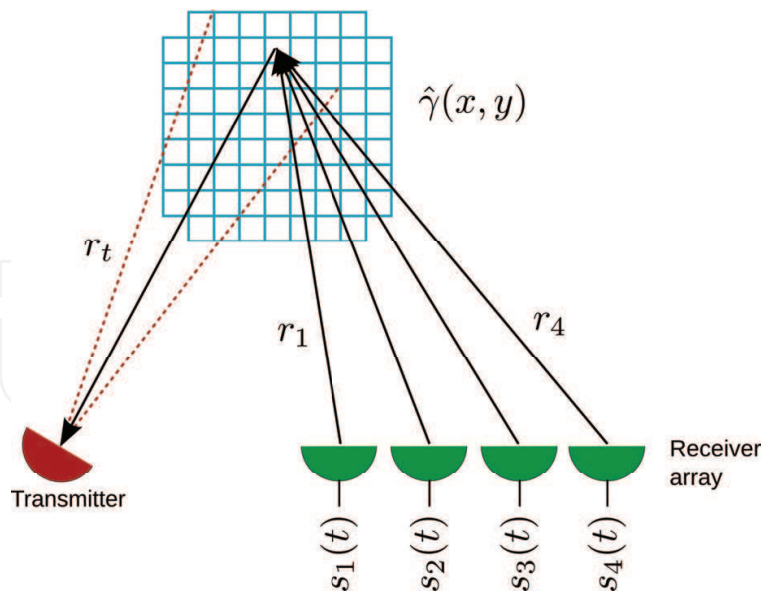
Fig. 3. Backprojection geometry.

backprojection is also closely related to Kirchhoff migration in seismic processing (Claerbout, 1995). Formally, backprojection is straightforward and can be done as follows. First the signals in each receiver are filtered and pulse compressed. Then the signal from each receiver is delayed to the pixel of interest

$$t_n(x,y) = (r_t + r_n)/c. \tag{1}$$

where r_t is the distance from the transmitter to the pixel, r_n is the distance from the pixel to receiver n, and c is the sound velocity. Then the recorded, pulse compressed signals s_n are summed coherently over all receivers to produce an estimate of the reflectivity function

$$\hat{\gamma}(x,y) = \frac{1}{N} \sum_{n=1}^{N} A_n s_n(t_n(x,y)). \tag{2}$$

The amplitude A_n is generally a function of geometry and frequency $A_n = A_n(r_t, r_r, \omega)$. In addition, the direction dependent sensitivity of the receivers can be taken into account. This amplitude factor can also be used to control the sidelobe suppression vs the angular resolution (Van Trees, 2002). For sampled time series $s_n(t_n(x,y))$ may have to be interpolated to obtain accurate values in the image. A simple algorithmic description of the backprojection algorithm is shown in Listing 1. We immediately realise why this method is called *Delay-And-Sum*. The signals are delayed to the correct pixel, and then summed.

2.2 Angular resolution

The *angular resolution* can be defined as the minimum angle for which two reflectors can be separated in the sonar image. A very simple and intuitive way to derive this is as follows. Assume a phased array receiver of length L consisting of a number of elements as illustrated in Fig. 4. The angular resolution for this receiver is the angle difference for which the echo from two reflectors gives destructive interference in the receivers. Consider a reflector at broadside and a reflector at an angle $\beta/2$. As the maximum range difference will always be on the ends of the array, we only consider the center element and the end element displaced $L/2$ apart. The distance difference between these two reflectors is

$$\delta R = R_0 - R_1. \tag{3}$$

```
for all directions
    for all ranges
        for all receivers
            Calculate the time delay
            Interpolate the received time series
            Apply appropriate amplitude factor
        end
        sum over receivers and store in gamma(x,y)
    end
end
```

Listing 1. Backprojection Pseudo-code

For range differences larger than $\delta R = \lambda/4$ destructive interference will start to occur. The difference in range is

$$\delta R = R_0 - R_1 = L/2 \sin(\beta/2). \tag{4}$$

We define β as the *angular resolution* and solve for when destructive interference will start

$$\delta R = L/2 \sin(\beta/2) = \lambda/4. \tag{5}$$

For small angles, we can approximate the sin-function

$$L/2\beta/2 = \lambda/4 \Rightarrow \boxed{\beta = \frac{\lambda}{L}}. \tag{6}$$

Hence, the angular resolution (in radians) equals the inverse length of the array measured in wavelengths. A longer array or a higher frequency (shorter wavelength) gives better angular resolution. More details and a more accurate derivation of angular resolution can be found in (Van Trees, 2002).

2.3 Imaging techniques for phased arrays

Fig. 5 shows the basic imaging geometry for an array of receivers (a phased array). The field of view is defined by the beamwidth of each of the receivers and their look direction. The
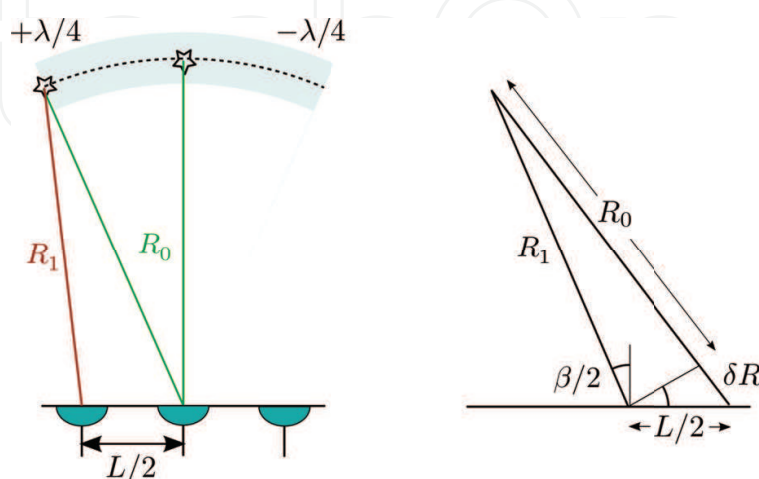

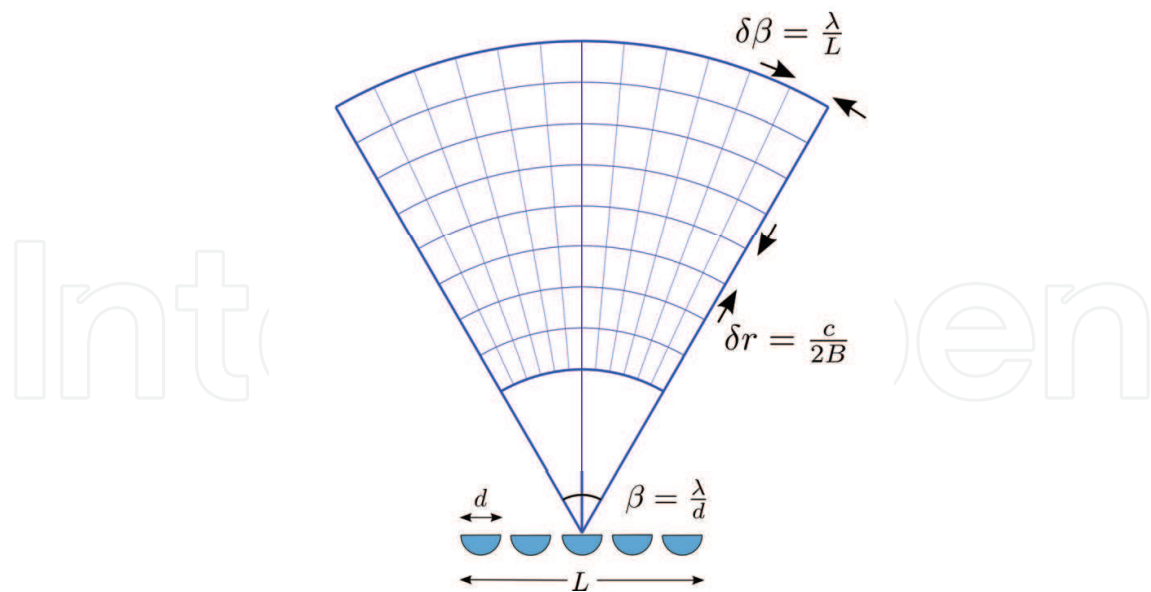Fig. 4. Geometrical derivation of angular resolution.

Fig. 5. Field of view and resolution in imaging sonar.

angular resolution is given by the array length and the wavelength. If the individual elements are more than $\lambda/2$ apart, the directivity of each element must be small enough to mitigate alias lobes (see section 3.1). For an active system, the range resolution is defined by the bandwidth of the system. The maximum range is determined by the pulse repetition interval and/or the sensitivity of the receiver elements. For a linear array it can be fruitful and efficient for the imaging to define a polar coordinate system fixed to the sonar.

In underwater applications, beamforming can be used to produce different types of products. For high frequency sonar imaging, this can be categorized into three different types, as illustrated in Fig. 6:

Sectorscan sonar produces a two-dimensional image for each pulse. These images are usually shown on a display pulse by pulse. Sectorscanning sonar is often used as hull mounted sonars for forward looking imaging or wide swath imaging. In fisheries acoustics, some cylindrical arrays actually produce full 360 degrees view.

Sidescan sonar is a particular type of sonar that uses the platform motion to cover different parts of the seafloor. A sidescan sonar produces one or a few beams around broadside, and an image of the seafloor is produced by moving the sonar and using repeated pulses. This is a very popular technology, it has fairly low hardware complexity and can therefore be more affordable. There are several books covering sidescan sonar very thoroughly (Blondel, 2009; Fish & Carr, 2001).

Synthetic aperture sonar uses multiple pulses to create a large synthetic array (or aperture). From this, an image of the seafloor is produced such that the information from multiple pulses goes into each pixel on the seafloor. It is, from a certain point of view, the combination of sidescan sonar and sectorscan sonar.

3. SAS sampling and coverage rate

In all types of array signal processing, the sampling of the array, or the spacing of the elements and their directivity, is critical. If the array is too sparsely sampled, grating or alias lobes will
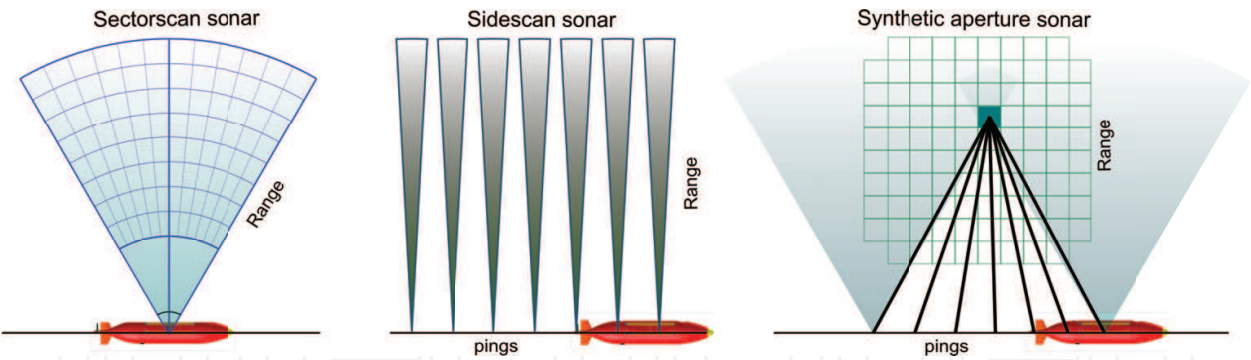
Fig. 6. Phased array imaging concepts for sonar.

occur, and the image quality will be reduced. In this section we describe the sampling criterion and show how this affects SAS design.

3.1 Undersampling of arrays

Consider a simple array with two elements displaced D apart, as illustrated in Fig. 7. Assume an inbound plane wave at broadside $\theta = 0$ with wavelength λ from a reflector in the far field. Any plane wave coming in the direction

$$\sin \theta_n = \pm n \frac{\lambda}{2D} \tag{7}$$

where n is an integer, will be perfectly in phase with the plane wave at broadside. Note that the factor two, i.e. $\lambda/2$, comes from assuming two-way propagation (transmission and reception). This ambiguity will cause grating lobes or alias lobes in the beampattern (Manolakis et al., 2000; Van Trees, 2002). To avoid grating lobes, the beamwidth of each individual element must be smaller than the distance to the first grating lobe. Assuming that each element is of size d with a beamwidth of $\beta \approx \lambda/d$, we get the sampling criterion

$$D \leq d/2. \tag{8}$$

Hence, for a well sampled array, the effective distance between each element must be half the size of each element. This is fulfilled for a densely populated array without gaps between elements (see below).

Grating lobes are such that the problem they cause cannot be fixed in signal processing afterwards. For linear uniform arrays (ULAs), there is a deterministic and simple one-to-one
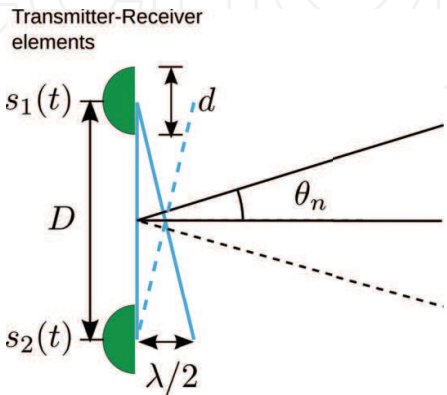

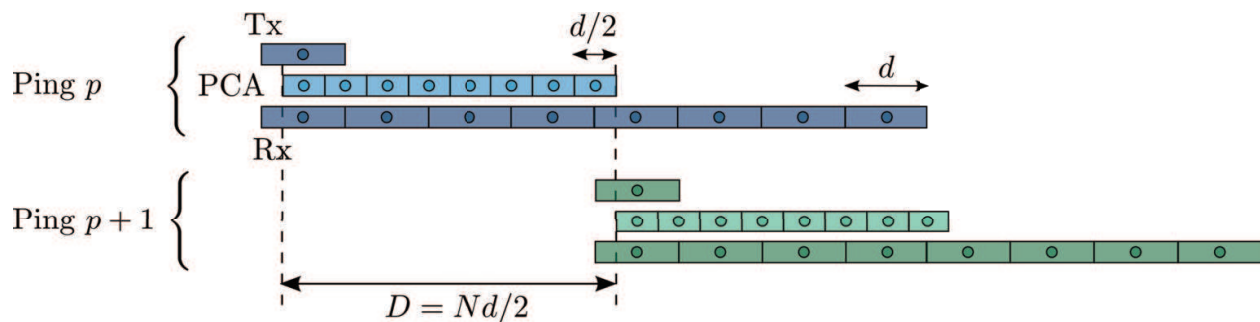Fig. 7. Along track sampling and grating (alias) lobes.

Fig. 8. Multi-element receiver array and the Phase Center Approximation.

relation between the sampling of the array and the angular position of the grating lobes. Grating lobes are frequency dependent. For large bandwidth systems, the grating lobes will be less defined due to the fact that their positions change with frequency.

3.2 Multi-element receiver arrays in SAS

In SAS, the transmitter-receiver pair is moved along-track and pulsed repeatedly to form a long synthetic antenna. The sampling criterion (8) imposes a maximum allowed displacement between pings, which again, transforms into a maximum range for a given speed. The maximum range R_{max} is given by

$$2R_{max}/c = T_{pri} = D/v \quad \Rightarrow \quad R_{max} = \frac{cD}{2v} \tag{9}$$

where v is the platform speed and T_{pri} is the pulse repetition interval. This relation imposes a very strong limitation to SAS. Consider a platform speed of $v = 2\,\text{m/s}$. For a displacement of $D = 5\,\text{cm}$, the maximum range then becomes $R_{max} = 18.75\,\text{m}$ for a sound velocity of $c = 1500\,\text{m/s}$. This is an unacceptable small range for most applications. To overcome this, a receiver array of multiple elements can be used (Bruce, 1992; Cutrona, 1975). The multi-element receiver array is used in almost all existing SAS systems today.

A simple description of how a single transmitter multiple receiver system can be used to form a synthetic aperture is as follows. Consider a single transmitter Tx and N receivers of size d in a linear array Rx, as illustration shown in Fig. 8. In stead of treating this as a bistatic system with one transmitter and many receivers, we assume a virtual array where each element is placed at the middle position between each transmitter-receiver pair (indicated in light green). In this array, each element is a transmitter-receiver (monostatic). This is the Phase Center Approximation (PCA) (Bellettini & Pinto, 2002). The virtual array (or PCA array) is half the length of the receiver array, with element size $d/2$, and each of the elements in the virtual array can be placed directly in a synthetic array (similar to SAR). The maximum displacement between two pulses becomes the length of the PCA array $D = Nd/2 = L/2$, and the maximum range becomes

$$R_{max} = \frac{cL}{4v} \tag{10}$$

where L is the length of the receiver array. The maximum range can then be increased by increasing the length of the receiver array. Fig. 9 shows the maximum range as function of vehicle speed for three different receiver array lengths. Note that the area coverage rate (speed times range) is a constant proportional to the array length.

In airborne SAR, aperture undersampling is not a problem, since the phase velocity for electromagnetic waves in air is relatively high compared to the platform speed. In large
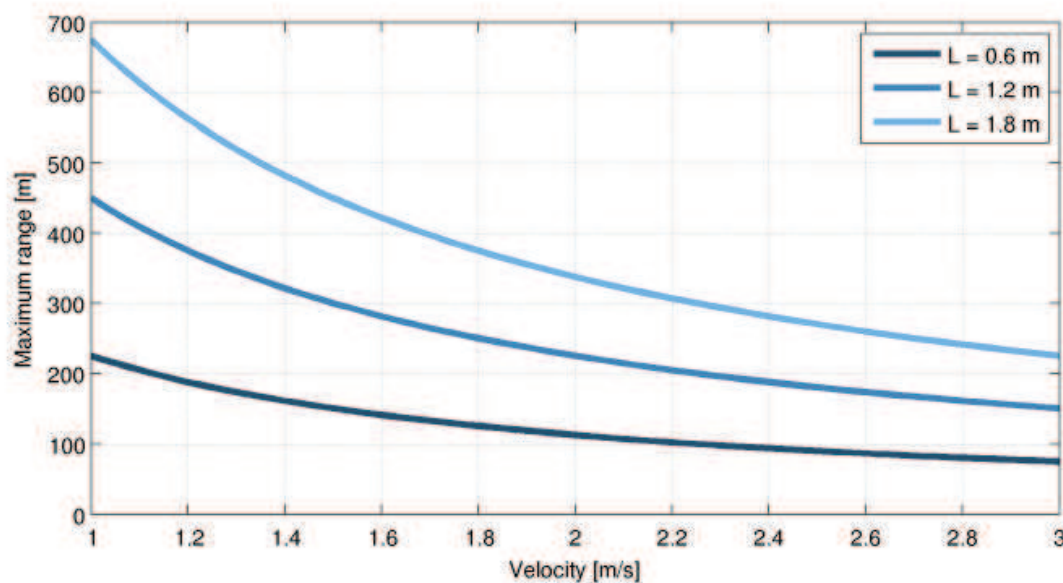
Fig. 9. Maximum range for given platform speed for three different receiver array lengths.

swath high resolution space-borne SAR, there is a limitation related to the sampling criterion. Advanced SAR systems have 2D phased arrays and use electronic steering of the transmitter and receiver arrays for different SAR modes. ScanSAR (Franceschetti & Lanari, 1999) and *Terrain Observation by Progressive Scans* (TOPS) (Gebert et al., 2010) are used to increase the area coverage rate while lowering the resolution. Spotlight mode (Jakowatz et al., 1996) is used to increase the resolution while lowering the area coverage rate.

4. Design of Synthetic Aperture Sonar

SAS is different from traditional sonar in several ways. In this section we describe some of the significant differences that affect the performance and application areas of SAS.

4.1 Resolution
While traditional imaging sonar has constant angular resolution, and thereby range dependent along-track resolution, SAS produces range independent along-track resolution. This is done by increasing the length of the synthetic array as function of range. Consider the left illustration of Fig. 10. The maximum length of the synthetic aperture is given by the field of view of each transmitter/receiver element. At range R_1, the length of the synthetic aperture becomes

$$L_1 \approx \beta R_1 \tag{11}$$

where $\beta = \lambda/d$ is the field of view. The along-track resolution is given by the synthetic antenna

$$\delta x \approx R_1 \frac{\lambda}{2L_1} \tag{12}$$

where the factor 2 comes from the fact that both the transmitter and receiver is moved along the synthetic aperture (creating a focused receiver and transmitter). Inserting for L_1 and β we get a resolution of

$$\delta x \approx R_1 \frac{\lambda}{2L_1} = R_1 \frac{\lambda}{2\beta R_1} = R_1 \frac{\lambda}{2\lambda/dR_1} = \frac{d}{2}. \tag{13}$$
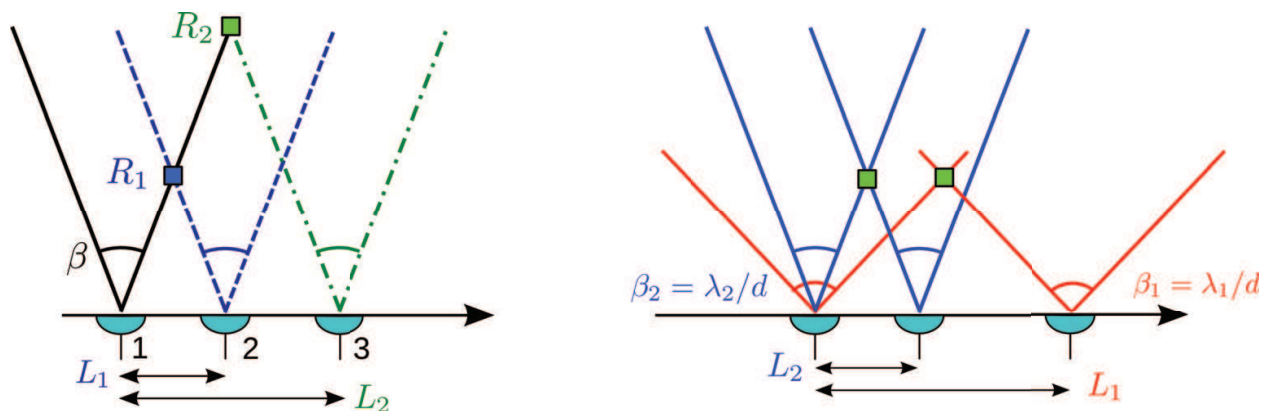
Fig. 10. Left: Range independent along-track resolution in SAS. Right: Frequency independent along-track resolution in SAS.

Hence, the along-track resolution for full length synthetic apertures is given by the element size alone, independent of range. This is a well known result, and there are numerous books covering this (Curlander & McDonough, 1991; Franceschetti & Lanari, 1999). This gives a degree of freedom not available in traditional sonar, where the cross-range resolution inevitably decreases with increasing range.

The length of the synthetic aperture is range dependent. Consider again the left drawing in Fig. 10. At range R_2, the length of the synthetic aperture becomes L_2 to obtain the same along-track resolution as for range R_1. The image quality becomes range dependent, since the transmission loss (Lurton, 2010) and thereby the Signal to Noise Ratio (SNR) is range dependent. Since the synthetic aperture is longer at longer range, the required accuracy in navigation, sound velocity and topography becomes thougher (see section 5). Hence, SAS at long range is inherently more difficult than SAS at short range.

4.2 Frequency dependence

Another intriguing fact is that SAS provides frequency independent along-track resolution. This is achieved by increasing the length of the synthetic aperture for decreasing frequency. The right drawing in Fig. 10 illustrates this. The lower frequency (red curve) requires a longer synthetic aperture than the higher frequency (blue curve) for a fixed resolution. The angular spread, however, becomes frequency dependent. For lower frequency SAS, larger angular spread is needed for a given along-track resolution. There is a lower limit to the resolution, where (13) does not hold. The best possible along-track resolution that can be achieved is $\delta x = \lambda/4$, for 180° field of view.

The frequency independence gives a degree of freedom compared to traditional sonar. Seawater is a dissipative medium for acoustic waves through viscosity and chemical processes (Brekhovskikh & Lysanov, 1982, pages 9-11), (Lurton, 2010, pages 23-27), (Medwin & Clay, 1998, pages 104-110). Acoustic absorption in seawater is frequency dependent, such that lower frequencies reach longer than higher frequencies. Fig. 11 shows the two-way transmission loss for some typical frequencies used in high frequency sonar imaging. For a given reception threshold (sensitivity), the maximum achievable range changes substantially. In traditional sonar, a typical design criterion is to choose the highest possible frequency for the desired range. Then design the transmitter and receiver arrays to obtain best possible azimuth resolution. In SAS, the along-track resolution is independent of frequency. This allows the center frequency to be chosen for other reasons than resolution.
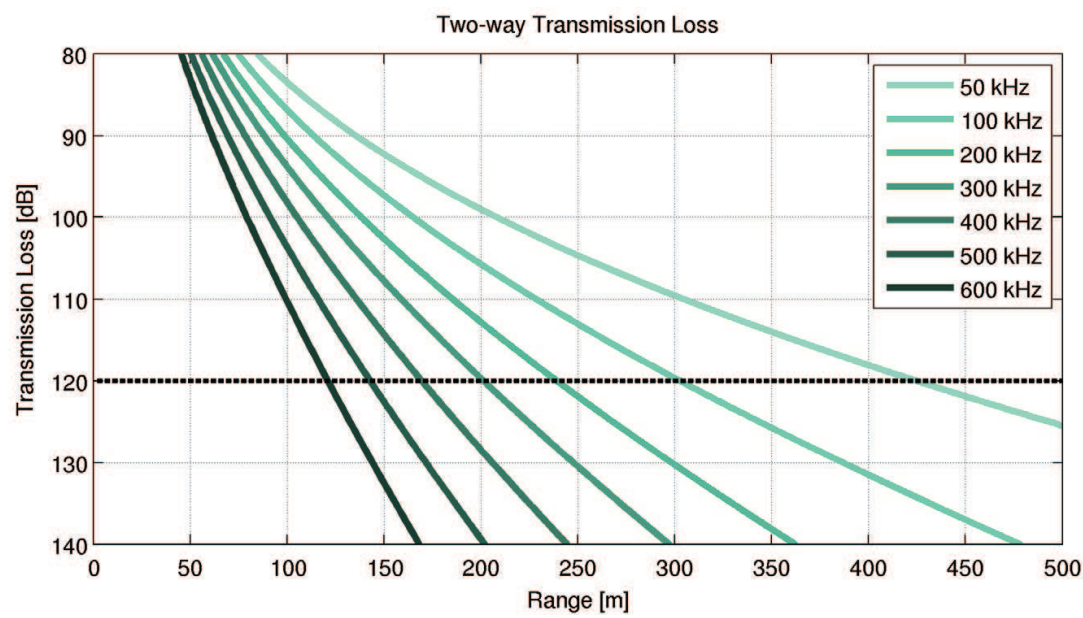
Fig. 11. Two-way transmission loss for typical frequencies in SAS.

4.3 Design parameters

There are many different SAS designs based on different philosophies. Here, we list some systems to illustrate the variety in existing designs. In (Bellettini & Pinto, 2009), the sonar has a center frequency of 300 kHz, and a receiver array length of 1.2 m with 36 elements. This sonar was designed to have a maximum range of 200 m at 2 m/s, good shallow water performance and as little angular spread as possible on the targets. In (Larsen et al., 2010), the center frequency is 60 kHz, and the receiver array is 4.3 m with 32 elements and a maximum range is 1500 m at 1 m/s speed. This system was specifically designed for deep tow with very large swath. The system described in (Jean, 2008) has a center frequency of 100 kHz, a receiver array of length 2 m with 24 elements, giving a maximum range of 300 m at 2.5 m/s speed. The system described in (Glover & Campell, 2010) is a dual frequency SAS at 17.5 kHz and 150 kHz, with a receiver array of 0.6 m length and 24 receiver elements. This gives a maximum range of 100 m at 2 m/s speed. The system described in section 8.1 has a center frequency of 100 kHz and a receiver length of 1.2 m with 32 elements, giving 200 m range at 2 m/s speed.

In Table 1 we list some design parameters (left column) and what controls these (right column). The general rule of thumb is that higher performance in resolution and area coverage rate requires more hardware, more processing capability and thereby also more space and power consumption (as expected). A slightly less obvious conclusion is that a high resolution system inherently is more robust. The future will surely bring new designs as the frequency agility of transducers improves, and the ability for large number of channels increases.

5. Challenges in SAS

The principle of SAS has been known in more than 40 years (Gough & Hawkins, 1998; Hayes & Gough, 2009), but it is only the last few years SAS has become commercially available. The main reason for this is the specific challenges that has to be solved for successful SAS imagery. In this section, we list some fundamental challenges and indicate how these can be solved. More details can be found in (Hagen & Hansen, 2008; 2009; Hansen, 2010; Hansen, Callow, Sæbø & Synnes, 2010).

Design Parameter	Relation
Range resolution	System Bandwidth
Along-track resolution	Element size
Area coverage rate	Receiver array length
Maximum range	Frequency, receiver array length and speed
Signal to Noise Ratio	Frequency, geometry and maximum range
Robustness	Relative bandwidth and redundancy
Complexity	Beamwidth, number of elements and relative bandwidth
Throughput	Bandwidth times number of receiver elements

Table 1. Design parameters and their relation in SAS.

5.1 Navigation

The sonar has to be positioned with accuracy better than a fraction of a wavelength along the synthetic aperture. This is the same requirement as for any other array sensor, but inherently more difficult to obtain since a synthetic antenna is formed by a moving platform. A sharp image depends on accurate positioning of the elements in the array. How much error is tolerated is dependent on the scale of the error and the required image quality (Carrara et al., 1995). Navigation of underwater platforms is more difficult than navigation of airborne and terrestrial platforms because GPS is not available. This challenge is the most important, and the first that has to be overcome for successful SAS imagery.

One solution is to use the sonar data itself for navigation (referred to as *micronavigation*). Compare the illustration in Fig. 12 with Fig. 8. By moving the SAS system a distance $D = Md/2$ such that $M < N$, there will be redundancy (or overlap) in the synthetic aperture. The overlap in the phase center antenna (PCA) is indicated in orange. Estimating which channels overlap can be used to estimate the displacement along-track and cross-track. This can be done by cross correlating the data recorded by elements from ping p with data recorded by other elements from ping $p + 1$. The method is named displaced phase center antenna (DPCA) or redundant phase center (RPC). DPCA was first used in Moving Target Indicator (MTI) radars in the 1950s (Dickey Jr et al., 1991). In SAS, early descriptions of DPCA can be found in (Pinto et al., 1997; Sheriff, 1992). A very good overview of the method is given in (Pinto, 2002), and a detailed study of the performance is given in (Bellettini & Pinto, 2002). In (Hansen et al., 2003) different strategies to combine DPCA with traditional inertial navigation is described.

Micronavigation using DPCA causes a trade-off between navigation performance and efficiency (area coverage rate). This is due to the fact that the displacement between pings has to be less than the maximum displacement $L/2$. More overlap gives better navigation but lower area coverage rate. An exception to this is if several transmitters, specific bandwidth, and a specific pulse regime is used (Billon & Fohanno, 2002).

5.2 Topographic errors

When running a vehicle on a non-straight track, a non-straight synthetic aperture is formed and the imaging geometry becomes dependent on the full three-dimensional geometry. This means that the position of the sonar has to be known and the topography (or bathymetry) of the scene to be imaged has to be known (Jakowatz et al., 1996, pages 187-197). Only then, successful SAS processing can be done. This is critical for robust SAS, and a significant problem since the topographic changes in rough terrain may impose severe non-linear tracks (Hansen et al., 2009). There are two solutions to this challenge: either run on a straight line or
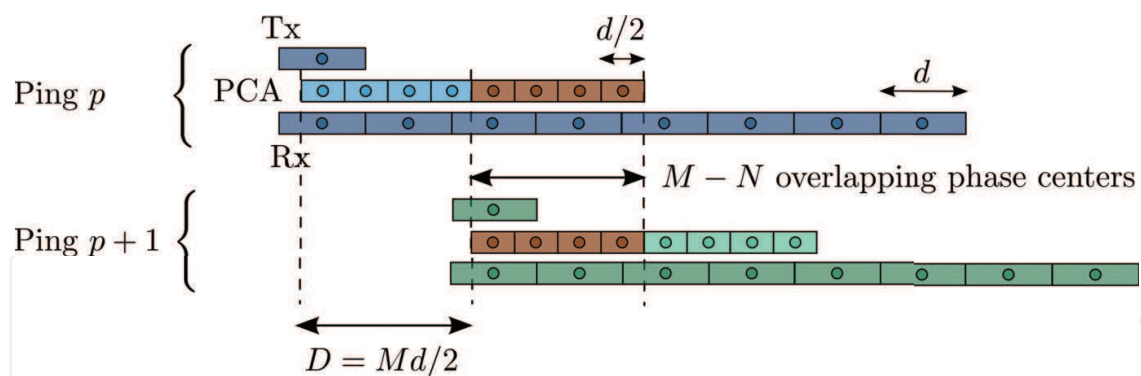
Fig. 12. Multi-element receiver array and the principle for Displaced Phase Center Antenna.

obtain a map of the area before synthetic aperture processing. The former is impractical (or impossible) on small platforms such as autonomous underwater vehicles (AUVs) or towfish systems. The latter can be obtained by using an interferometric sonar to map the scene prior to SAS processing.

5.3 Ocean environment

SAS is near-field imaging. This implies that the sound velocity has to be accurately estimated for well focused imaging. The sound velocity in the ocean varies with depth (Brekhovskikh & Lysanov, 1982, pages 1-9), (Lurton, 2010, chapter 2.6). There might also be local horizontal and temporal variations. This can cause variation in the sound velocity of up to 2% along the acoustic path. The effect of incorrect sound velocity on SAS is described in (Hansen et al., 2007; Hansen, Callow, Sæbø & Synnes, 2010). To overcome this, the sound velocity can be measured directly or calculated using a Conductivity, Temperature, Depth (CTD) sensor. Another possibility is to auto correct for incorrect sound velocity by using an autofocus technique (Hansen et al., 2007; Jakowatz et al., 1996).

5.4 Vehicle stability

SAS systems are generally multi-element receiver systems (see section 3.1). This affects synthetic aperture processing in several ways. For vehicles operated in a crabbing environment (where the heading is not aligned with the track), a baseline occurs between overlapping elements. Even if the track is perfectly linear, the synthetic aperture becomes non-linear and the image quality in SAS processing becomes dependent on the topography accuracy (see section 5.2). Large crab-induced baselines is challenging for imaging and also micronavigation (Callow, 2010).

5.5 Multipath environment

When operating in shallow waters, multiple reflections (or multipath) via the sea surface might affect the performance of sonar (Lurton, 2010, chapter 2.4), (Bellettini et al., 2003). This can affect the SAS data threefold: Multipath can potentially lower the temporal coherence between pings in the micronavigation; multipath can reduce the spatial coherence in interferometry; and multipath can add unwanted signal to the SAS images, causing loss of shadow contrast and fidelity. The latter two problems applies to all sonars in shallow waters, not only SAS. How much the shallow water environment affects SAS is actually dependent of the seafloor conditions, the sound velocity profile and the sea surface roughness (Synnes et al., 2009).
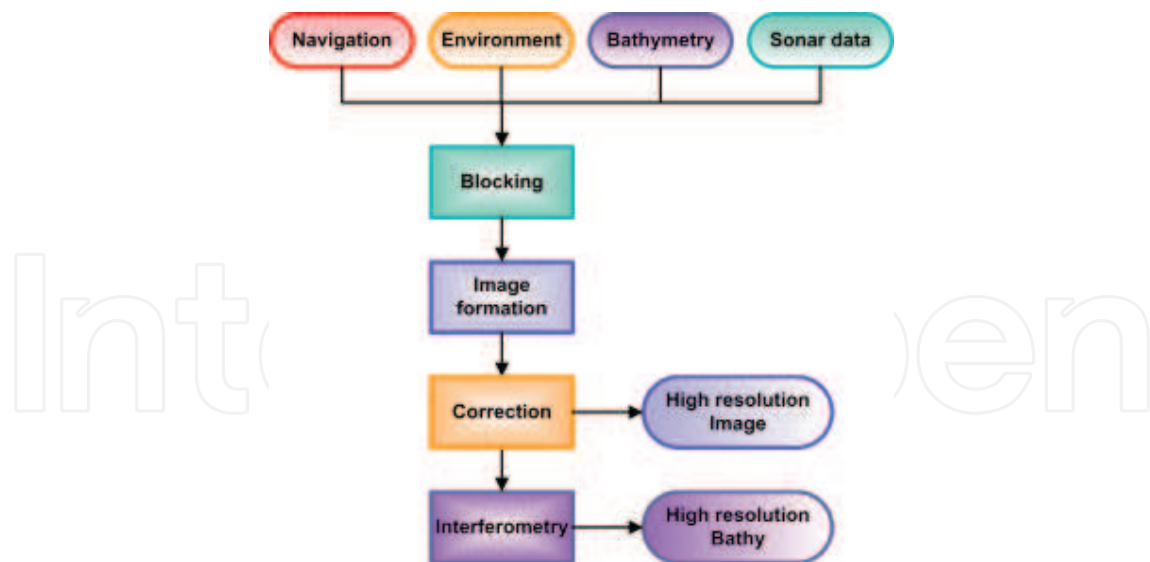
Fig. 13. Overview of SAS signal processing flow.

6. Signal processing of SAS data

Signal processing of SAS data can be done in many different ways. Fig. 13 shows the shcematic overview of a processing flow. Signal processing of SAS data is similar to SAR processing, with a few exceptions. Accurate knowledge of the vehicle navigation (track position and sensor orientation), the ocean environment and in particular the sound velocity, and the seafloor topography must be obtained for successful SAS imagery (see section 5).

The first step (blocking) in the processing is to divide the data into portions suitable for synthetic aperture processing. The blocking selects which pings to put into one synthetic aperture, and decides what to do with the data. If micronavigation is required, this must take place before imaging. There are two classes of image formation algorithms: time domain imaging and frequency domain imaging. In general, the frequency domain algorithms are more efficient but require more controlled vehicle behavior (close to straight line tracks). Candidates are the wavenumber algorithm (Soumekh, 1994),(Cumming & Wong, 2005, chapter 8), (Carrara et al., 1995, chapter 10) (also referred to as range migration algorithm or Omega-K algorithm), and the chirp scaling algorithm (Cumming & Wong, 2005, chapter 7), (Franceschetti & Lanari, 1999). Alternatively, the image formation can be done in time domain (see section 2.1). An overview of different algorithms used in SAS imaging can be found in (Gough & Hawkins, 1997).The benefit of time domain beamforming is that the imaging grid can be arbitrary and the data acquisition (the synthetic aperture) can be severely distorted. This gives an added flexibility not available in frequency domain imaging (Massonnet & Souyris, 2008, chapter 2.4). The disadvantage of time domain imaging is the computational load. After image formation, blind correction for residual errors (known as autofocus) in the image can be performed (Jakowatz et al., 1996, chapter 4), (Callow, 2003). It should be noted that most autofocusing techniques are local methods - they have a certain success in correcting local errors, but do not perform well on a large image with different sources for errors in different locations in the image. For interferometric systems, the final stage in the SAS processing flow is bathymetry estimation using interferometry (Hanssen, 2001; Sæbø, 2010).

7. Properties of SAS images

The goal of sonar imaging is to estimate the acoustic reflectivity in the best possible manner, given the sensor and geometry (see section 2). (Oliver & Quegan, 1998) gives an excellent overview of the properties of SAR images (highly relevant for SAS), related to the signal processing and the scene content. In the following, we list common measures of system performance, applicable to any imaging system.

Geometrical resolution or detail resolution. This is the minimum distance between two reflectors where they can be resolved in the image. The theoretical geometric resolution is given by the bandwidth for the range dimension and the element size for the along-track dimension (see section 4.1). The true geometrical resolution is also dependent on the image quality. Defocus will reduce the geometrical resolution (Oliver & Quegan, 1998, chapter 3.2).

Radiometric resolution or contrast / value resolution, echogenicity or target strength accuracy. This is the accuracy of the estimated value in each pixel. All coherent imaging systems suffers from speckle (Goodman, 2007; Oliver & Quegan, 1998). Speckle is random variability caused by constructive and destructive interference between individual scatterers in each geometrical resolution cell. Speckle causes a variance in the pixel value and thereby a reduced radiometric resolution. There are different methods to despeckle images and to estimate the scattering cross section. The traditional approach in SAR has been to apply multilook processing to reduce speckle (Jakowatz et al., 1996, chapter 3.3). There also exist more advanced methods to estimate the scattering cross section (Massonnet & Souyris, 2008, chapter 3.11), (Oliver & Quegan, 1998, chapter 6). The radiometric resolution strictly depends on a fully calibrated system, where the whole system has to be energy preserving. This is non-trivial to obtain, and it implies that all the terms except the Target Strength in the sonar equation has to be accounted for (Ainslie, 2010; Lurton, 2010), (Curlander & McDonough, 1991, chapter 7).

Dynamic range or resolvability of small targets in the presence of large targets. This is a function of the sidelobe levels or the shape of the point spread function. There is a trade-off between geometrical resolution and dynamic range. Large dynamic range requires large sidelobe suppression which causes poorer geometrical resolution (Franceschetti & Lanari, 1999, chapter 3.1), (Carrara et al., 1995, chapter 8). In addition to the sidelobes, the alias lobes (or grating lobes) must also be controlled in order to obtain the desired dynamic range. This can only be achieved by oversampling the synthetic aperture (Bellettini & Pinto, 2009; Gough & Hawkins, 1997).

Sensitivity or detection ability of low level targets. This is determined by several of the terms in the sonar equation (Lurton, 2010; Urick, 1983), such as system self noise, transmit power, transmission loss (which is a function of acoustic frequency) and processing gain. See (Ainslie, 2010) for a detailed description of the terms in the sonar equation. A system with larger pulse compression gain will have improved sensitivity.

Temporal resolution or framerate. This is the number of independent images on the scene per unit time. Since SAS is based on space-time processing (spatial movement uses time to generate aperture), SAS only has one frame on the scene when using full aperture length. Multi-aspect imaging (Hansen et al., 2008) can be applied to produce multiple aspects from different apertures and thereby different time intervals. There is a trade-off between looks and along-track resolution (since the aperture becomes shorter).
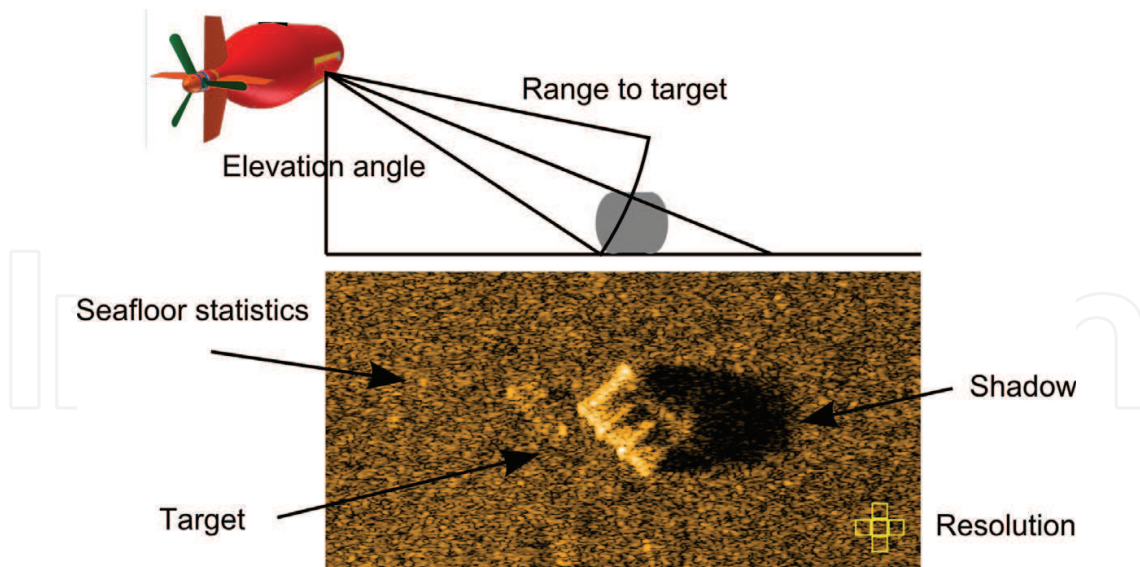
Fig. 14. The ability to retrieve relevant information from a SAS image is dependent on a number of different factors.

The ability to extract the relevant information from a SAS image depends on a number of different factors, as illustrated in Fig. 14. Observation geometry given by range and elevation angle is important for interpretation of the highlight structure and shadow. Backscattered target signals can contain elements of specular reflections, diffuse scattering, transparency, resonant scattering and multiple scattering, all of which complicate the process of retrieving the relevant information. Finally, image resolution is critical in resolving or classifying objects, shadow shape and the surrounding scatterers on the seafloor.

8. Applications of SAS

There are many applications where SAS is suitable. Very high resolution acoustic imaging can be achieved on traditional sonar using very high frequencies, and there are sonar systems today using up to 2 MHz frequency. They are, hovewer, very limited in range. When large area coverage *and* very high resolution is needed at the same time, SAS is really the only technology that can provide a solution. In this section, we describe a particular SAS system, the HISAS 1030, and show example images from different applications.

8.1 The HISAS 1030 interferometric SAS

HISAS 1030 is a wideband widebeam interferometric SAS developed by Kongsberg Maritime and FFI (Fossum et al., 2008; Hagen et al., 2008). The sonar contains two along-track receiver arrays of 1.2 m length with 32 elements in each array, and a vertical baseline approximately 30 cm which equals 20 wavelengths. The transmitter is a vertical phased array with 16 elements, and the transmit beam can be electronically steered and shaped to obtain the best possible performance in shallow waters (see Section 5.5). The transmitter can also be used as a receiver, giving 16 individual receiver channels along a vertical array. Fig. 15 shows the sonar mounted on a HUGIN 1000-MR AUV. Typical HISAS 1030 specifications are listed in Table 2. The SAS processing is done in a software suite named *FOCUS Toolbox* (Hansen et al., 2005; 2003).

Fig. 16 shows an example SAS image made by the HISAS 1030 on the HUGIN 1000 AUV. The image shows the wreck of the 1500 dwt oil tanker Holmengraa lying on a slanted seabed at
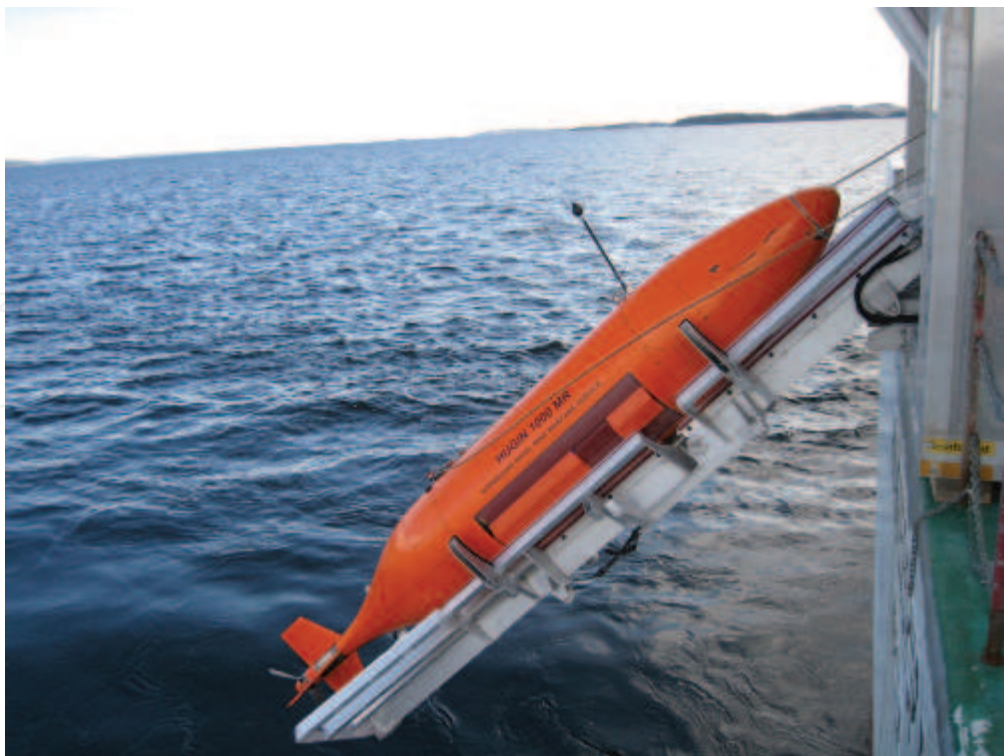
Fig. 15. The HISAS 1030 interferometric SAS on the HUGIN autonomous underwater vehicle. The picture was taken just before launch during a scientific mission on board the research vessel H U Sverdrup II in Norwegian waters in April 2010.

Center frequency	100 kHz
Wavelength	1.5 cm
Bandwidth	30 kHz
Total frequency range	50-120 kHz
Along-track resolution	3 cm
Cross-track resolution	3 cm
Maximum range @ 2 m/s	200 m
Area coverage rate	2 km^2/h

Table 2. Typical system specifications for the HISAS 1030 interferometric SAS.

depth 77 m. The distance to the center of the image is about 95 m. The length of the wreck is about 68 m and width about 9 m.

Fig. 17 captures the essence of SAS: Long range *and* high resolution at the same time. The large (middle) image shows a SAS image where the range is 25 m (left) to 325 m (right), and the dynamic range is 32 dB. The data was collected with HISAS 1030 on HUGIN AUV running at 2.3 knots at 40 m altitude, outside Horten, Norway in approximately 200 m water depth. The upper image shows a section from 200 m range to 250 m range with the wreck of the German WWII submarine U735. The lower image shows a section from 260 m range to 290 m range with a 1 m^3 cube. The length of the synthetic aperture is (see section 4.1)

$$L_{\text{sa}} \approx R\eta \frac{\lambda}{d} \qquad (14)$$

Fig. 16. SAS image of the wreck of the Norwegian tanker Holmengraa that was sunk during WWII in 1944. Courtesy of Kongsberg Maritime.

where R is the range, λ is the wavelength at center frequency, d is the along-track element size in the array. η is a programmable parameter controlling the *process beamwidth*, that is, the beamwidth actually processed. In this particular case, $\eta = 2/3$, and the length of the synthetic aperture at maximum range becomes $L_{sa} \approx 90\,\text{m} = 6000\lambda$. The SAS resolution-gain, defined as the ratio between along-track resolution in real aperture δx_{ra} and synthetic aperture δx_{sa} is

$$Q_{sa} = \frac{\delta x_{ra}}{\delta x_{sa}} = \frac{L_{sa}}{L/2} \approx R\eta \frac{2\lambda}{Ld}, \tag{15}$$

where and L is the array length. In Fig. 17, the SAS resolution-gain is $Q_{sa} \approx 150$ at maximum range. This is a considerable resolution improvement, and the equivalent along-track resolution is very difficult to obtain using real aperture techniques.

8.2 Underwater archaeology

SAS is a candidate technology in searching for wrecks and other objects of historic interest. Fig. 18 shows a SAS image collected by the Royal Norwegian Navy in a training mission close to the town of Tromsø in the winter of 2009. The data was collected at 34 m water depth, close to shore. The image shows the wreck of a German WWII Heinkel He 115 seaplane. The original length of the plane is 17 m and the wingspan was 22 m. Note the small part outside the right wing of the seaplane. This is probably one of the floats. The object in the lower left part of the image is probably the tail-section of another plane of the same type.
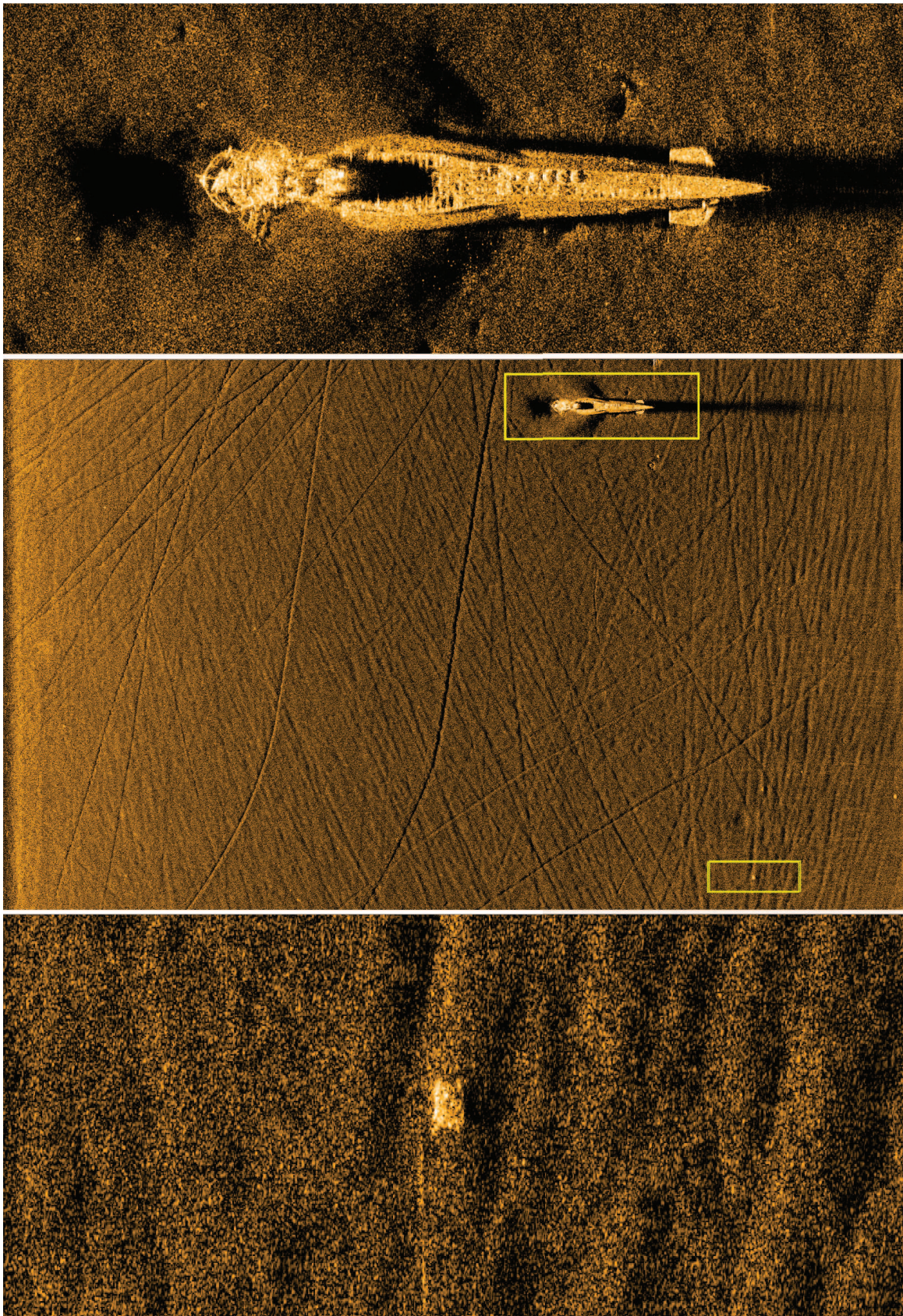
Fig. 17. Middle: SAS image where the range is 25 m (left) to 325 m (right). Courtesy of Kongsberg Maritime.

Fig. 18. SAS image of a German WWII Heinkel He 115 seaplane lying on the seafloor. Courtesy of the Royal Norwegian Navy. Photograph is from wikipedia.

8.3 Search for small objects

When searching for small objects over very large areas, SAS is an excellent tool. Fig. 19 shows a SAS image from an area with debris. The sonar has traveled along the vertical direction of the image, and the sonar look direction is towards right. The size of the image is 190 m (along-track) and 30 m to 165 m cross-track, and the water depth is around 70 m. The yellow boxes indicates three objects, and the small images below show zoomed images of the objects. These are two drums of approximate size 0.9 m length and 0.6 m diameter, and a cylinder of approximate length 2.5 m. The lower row of images shows optical images of the same objects. The optical images were collected with another HUGIN AUV. The altitude was 5 m on the data collection of the optical images. We see several interesting features in the objects. The drum at 73 m has clear indications of partial transparency. The back end of the barrel is clearly visible, and there is acoustic pollution in the shadow region. The drum at 112 m has a less defined back end and deeper shadow contrast, indicating that this object is less transparent. In the optical images, indeed, we see that the drum at 73 m has severe damage and holes, while the drum at 112 m looks to be more intact. In the optical image of the cylinder, we see a small cavity in the lower right end. This appears as a highlight in the SAS image.

30 m

165 m

Drum at 73 m   Drum at 112 m   Cylinder at 73 m
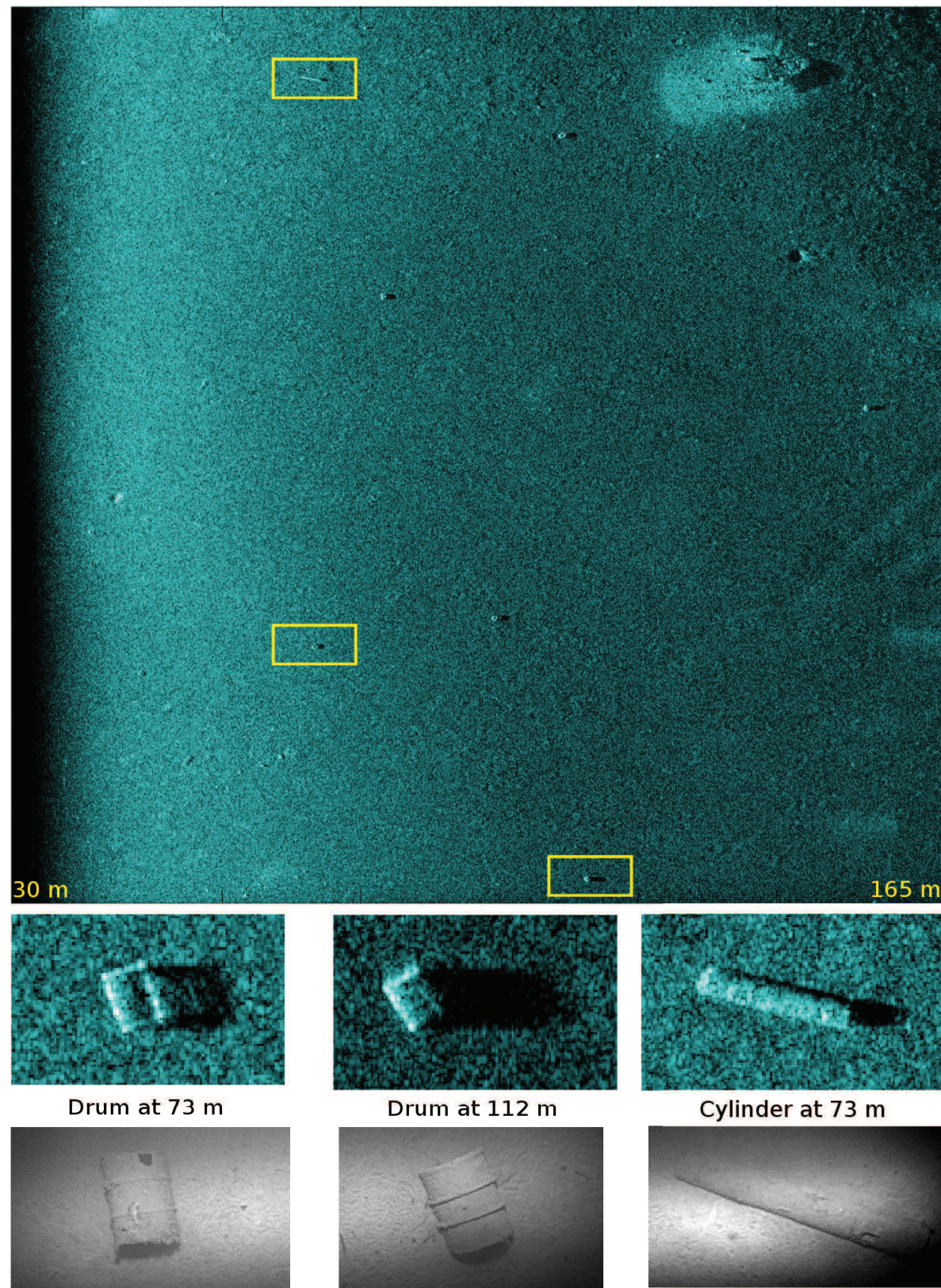
Fig. 19. Upper: SAS image of an area with small objects. The range is 30 m (left) to 165 m (right), and the along-track (vertical) is 190 m. The small cut-outs shows zoomed images of three different objects. The lower row shows optical images of the same targets. Courtesy of Kongsberg Maritime / FFI.

8.4 Inspection of man made constructions

External inspection of underwater constructions such as pipelines is an important task. The objective of these inspections is to detect burial, exposure, free spans and buckling of the pipeline, as well as possible damages due to trawling, anchoring and debris near the pipeline. SAS may be well suited technology for some of these tasks (Hagen et al., 2010), (Hansen, Sæbø, Callow & Hagen, 2010). Fig. 20 shows an example SAS image collected by a HUGIN AUV during a demonstration in San Diego, USA, in 2010. The image shows a sewer pipeline, and a rope or wire on the seafloor.

Fig. 20. Upper: SAS image of a pipeline outside San Diego. The range in the upper image is 65 m - 145 m. Lower: 20 m times 10 m zoomed area at range 85 m of a rope or wire on the seafloor. Courtesy of Kongsberg Maritime.

9. Conclusion

Synthetic aperture sonar (SAS) is an advanced signal processing technique to improve resolution in sonar imagery. The main application is detailed documentation of the seafloor, in areas such as search for small objects, underwater archaeology, detailed seabed mapping and documentation of underwater installations. Successful SAS is dependent on accurate knowledge about the sonar position, the ocean environment and the seabed topography.

SAS is substantially more mature now than 10 years ago. To illustrate the maturity of commercially available systems, we show a final example of SAS data collected by the HUGIN AUV carrying the HISAS 1030. Fig. 21 shows SAS images and interferometric SAS relative bathymetries of a German WWII Focke Wulf 190 A-3 aeroplane that was found by the Royal Norwegian Navy mine warfare flotilla. The length of the plane is 9 m and the wingspan is 10.5 m. The tail was damaged as we see in the SAS images and the bathymetries. The motor fell off during the recovery. These images was produced at sea by the Royal Norwegian Navy personnel during the search operation. The images was constructed using micronavigation and sidescan bathymetry as a preprocessing step, then backprojection in three dimensions for image formation, and finally bathymetry estimation using a maximum likelihood phase estimator in the interferometric processing.
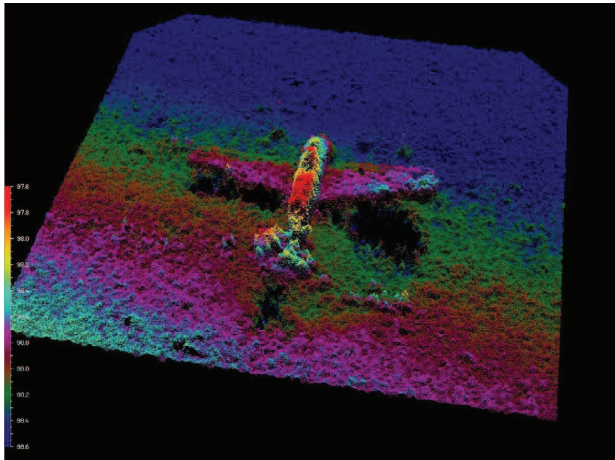
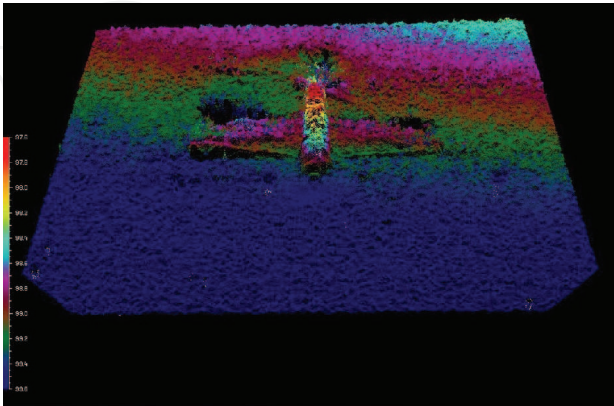## 10. Acknowledgments

(a) SAS image 1   (b) SAS image 2

(c) Bathymetry by SAS interferometry 1

(d) Bathymetry by SAS interferometry 2

(e) Photograph taken during the recovery
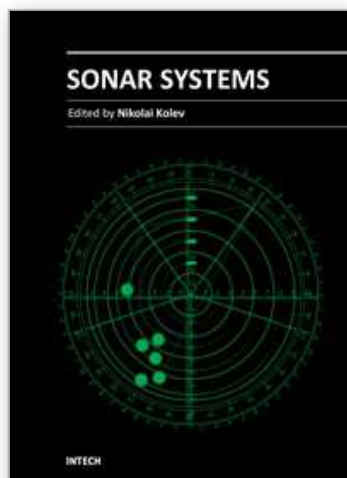

(f) Photograph taken during the recovery

Fig. 21. The German WWII Focke Wulf 190 A-3 aircraft. The plane was found by the Royal Norwegian Navy Mine warfare flotilla at 98 m water depth during an underwater archaeology mission. Courtesy of the Royal Norwegian Navy.

11. References

Ainslie, M. (2010). *Principles of Sonar Performance Modelling*, Springer Verlag.

Bellettini, A. & Pinto, M. A. (2002). Theoretical accuracy of synthetic aperture sonar micronavigation using a displaced phase-center antenna, *IEEE J. Oceanic Eng.* 27(4): 780–789.

Bellettini, A. & Pinto, M. A. (2009). Design and Experimental Results of a 300-kHz Synthetic Aperture Sonar Optimized for Shallow-Water Operations, *IEEE J. Oceanic Eng.* 34(3): 285–293.

Bellettini, A., Pinto, M. A. & Wang, L. (2003). Effect of multipath on synthetic aperture sonar, *Proc. 5th World Congr. Ultrasonics*, Paris, France, pp. 531–534.

Billon, D. & Fohanno, F. (2002). Two improved ping-to-ping cross-correlation methods for synthetic aperture sonar: theory and sea results, *OCEANS'02 MTS/IEEE*, Vol. 4, IEEE, pp. 2284–2293.

Blondel, P. (2009). *The Handbook of Sidescan Sonar*, Geophysical Sciences, Springer Praxis Books.

Brekhovskikh, L. & Lysanov, Y. (1982). *Fundamentals of Ocean Acoustics*, Vol. 8 of *Springer Series in Electrophysics*, Springer-Verlag, Berlin, Germany.

Bruce, M. P. (1992). A processing requirement and resolution capability comparison of side-scan and synthetic-aperture sonars, *IEEE J. Oceanic Eng.* 17(1): 106–117.

Burdic, W. S. (1984). *Underwater acoustic system analysis*, Prentice Hall.

Callow, H. J. (2003). *Signal Processing for Synthetic Aperture Sonar Image Enhancement*, PhD thesis, University of Canterbury, Christchurch, New Zealand.

Callow, H. J. (2010). Comparison of SAS processing strategies for crabbing collection geometries, *Proceedings of Oceans 2010 MTS/IEEE*, Seattle, US.

Carrara, W. G., Goodman, R. S. & Majewski, R. M. (1995). *Spotlight Synthetic Aperture Radar: Signal Processing Algorithms*, Artech House.

Claerbout, J. (1995). *Basic earth imaging*, Stanford Exploration Project.
      URL: *http://sepwww.stanford.edu/*

Cumming, I. G. & Wong, F. H. (2005). *Digital Processing of Synthetic Aperture Radar Data: Alogirthms and Implementation*, Artech House.

Curlander, J. C. & McDonough, R. N. (1991). *Synthetic Aperture Radar: Systems and Signal Processing*, John Wiley & Sons, Inc., 605 Third Avenue, New York, NY.

Cutrona, L. J. (1975). Comparison of sonar system performance achievable using synthetic-aperture techniques with the performance achievable by more conventional means, *J. Acoust. Soc. Am.* 58(2): 336–348.

Dickey Jr, F., Labitt, M. & Staudaher, F. (1991). Development of airborne moving target radar for long range surveillance, *Aerospace and Electronic Systems, IEEE Transactions on* 27(6): 959–972.

Fish, J. P. & Carr, H. A. (2001). *Sound reflections: Advanced Applications of Side Scan Sonar*, LowerCape Publishing.

Fossum, T. G., Hagen, P. E., Langli, B. & Hansen, R. E. (2008). HISAS 1030: High resolution synthetic aperture sonar with bathymetric capabilities, *Shallow survey*, Portsmouth, NH, USA.

Franceschetti, G. & Lanari, R. (1999). *Synthetic Aperture Radar Processing*, CRC Press.

Gebert, N., Krieger, G. & Moreira, A. (2010). Multichannel azimuth processing in ScanSAR and TOPS mode operation, *IEEE Trans. Geosci. Remote Sensing.* 48(7): 2994–3308.

Glover, N. P. & Campell, I. (2010). Simultaneous low and high frequency high resolution SAS and a statistical method of quantifying the resolutions obtained, *Proceedings of Synthetic Aperture Sonar and Radar 2010*, Lerici, Italy.

Goodman, J. W. (2007). *Speckle Phenomena in Optics: Theory and Applications*, Roberts and Company.

Gough, P. T. & Hawkins, D. W. (1997). Imaging algorithms for a strip-map synthetic aperture sonar: Minimizing the effects of aperture errors and aperture undersampling, *IEEE J. Oceanic Eng.* 22 (1): 27–39.

Gough, P. T. & Hawkins, D. W. (1998). A short history of synthetic aperture sonar, *Geoscience and Remote Sensing Symposium Proceedings, 1998. IGARSS'98. 1998 IEEE International*, Vol. 2, IEEE, pp. 618–620.

Hagen, P. E., Børhaug, E. & Midtgaard, Ø. (2010). Pipeline inspection with interferometric SAS, *Sea Technology* pp. 37–40.

Hagen, P. E., Fossum, T. G. & Hansen, R. E. (2008). HISAS 1030: The next generation mine hunting sonar for AUVs, *UDT Pacific 2008 Conference Proceedings*, Sydney, Australia.

Hagen, P. E. & Hansen, R. E. (2008). Synthetic aperture sonar challenges ... and how to meet them, *Hydro International* pp. 26–31.

Hagen, P. E. & Hansen, R. E. (2009). Robust synthetic aperture sonar operation for AUVs, *Proceedings of Oceans '09 MTS/IEEE Biloxi*, Biloxi, MS, USA.

Hansen, R. E. (2010). Robust synthetic aperture sonar for autonomous underwater vehicles, *Proceedings of Synthetic Aperture Sonar and Radar 2010*, Lerici, Italy.

Hansen, R. E., Callow, H. J. & Sæbø, T. O. (2007). The effect of sound velocity variations on synthetic aperture sonar, *Proceedings of Underwater Acoustic Measurements 2007*, Crete, Greece.

Hansen, R. E., Callow, H. J., Sæbø, T. O., Hagen, P. E. & Langli, B. (2008). High fidelity synthetic aperture sonar products for target analysis, *Proceedings of Oceans '08 Quebec*, Quebec, Canada.

Hansen, R. E., Callow, H. J., Sæbø, T. O., Synnes, S. A., Hagen, P. E., Fossum, T. G. & Langli, B. (2009). Synthetic aperture sonar in challenging environments: Results from the HISAS 1030, *Proceedings of Underwater Acoustic Measurements 2009*, Nafplion, Greece.

Hansen, R. E., Callow, H. J., Sæbø, T. O. & Synnes, S. A. V. (2010). Challenges in seafloor imaging and mapping with synthetic aperture sonar, *Proceedings of EUSAR 2010*, Aachen, Germany, pp. 540–543.

Hansen, R. E., Sæbø, T. O., Callow, H. J. & Hagen, P. E. (2010). Interferometric synthetic aperture sonar in pipeline inspection, *Proceedings of Oceans 2010 MTS/IEEE*, Sydney, Australia.

Hansen, R. E., Sæbø, T. O., Callow, H. J., Hagen, P. E. & Hammerstad, E. (2005). Synthetic aperture sonar processing for the HUGIN AUV, *Proceedings of Oceans '05 Europe*, Vol. 2, Brest, France, pp. 1090–1094.

Hansen, R. E., Sæbø, T. O., Gade, K. & Chapman, S. (2003). Signal processing for AUV based interferometric synthetic aperture sonar, *Proceedings of Oceans 2003 MTS/IEEE*, San Diego, CA, USA, pp. 2438–2444.

Hanssen, R. F. (2001). *Radar Interferometry: Data Interpretation and Error Analysis*, Kluwer Academic Publishers.

Hayes, M. P. & Gough, P. T. (2009). Synthetic aperture sonar: A review of current status, *IEEE J. Oceanic Eng.* 34(3): 207–224.

Jakowatz, J. C. V., Wahl, D. E., Eichel, P. H., Ghiglia, D. C. & Thompson, P. A. (1996). *Spotlight-Mode Synthetic Aperture Radar: A Signal Processing Approach*, Kluwer Academic Publishers.

Jean, F. (2008). Shadows, synthetic aperture sonar and forward looking gap-filler: different imaging algorithms, *Proceedings of OCEANS 2008 - MTS/IEEE Kobe Techno-Ocean*, Kobe, Japan.

Johnson, D. H. & Dudgeon, D. E. (1993). *Array signal processing: Concepts and Techniques*, Signal processing series, Prentice Hall, Englewood Cliffs, NJ, USA.

Larsen, L. J., Wilby, A. & Stewart, C. (2010). Deep ocean survey and search using synthetic aperture sonar, *Proceedings of Oceans 2010 MTS/IEEE*, Seattle, US.

Levanon, N. (1988). *Radar Principles*, Wiley Interscience.

Lurton, X. (2010). *An Introduction to Underwater Acoustics: Principles and Applications*, second edn, Springer Praxis Publishing.

Manolakis, D. G., Ingle, V. K. & Kogon, S. M. (2000). *Statistical and Adaptive Signal Processing*, McGraw-Hill.

Massonnet, D. & Souyris, J. (2008). *Imaging with synthetic aperture radar*, EFPL Press.

Medwin, H. & Clay, C. S. (1998). *Fundamentals of Acoustical Oceanography*, Academic Press, San Diego, CA, USA.

Nielsen, R. O. (1991). *Sonar signal processing*, Artech House.

Oliver, C. & Quegan, S. (1998). *Understanding Synthetic Aperture Radar Images*, Artech house, Inc.

Pinto, M. A. (2002). High resolution seafloor imaging with synthetic aperture sonar, *IEEE Oceanic Eng. Newsletter* pp. 15–20.

Pinto, M. A., Fohanno, F., Trémois, O. & Guyonic, S. (1997). Autofocusing a synthetic aperture sonar using the temporal and spatial coherence of seafloor reverberation, *in* O. Bergem & A. P. Lyons (eds), *High Frequency Acoustics in Shallow Water*, SACLANTCEN Conference Proceedings, NATO SACLANT Undersea Research Centre, La Spezia, Italy, pp. 417–424.

Sæbø, T. O. (2010). *Seafloor Depth Estimation by means of Interferometric Synthetic Aperture Sonar*, PhD thesis, University of Tromsø, Norway.

Sheriff, R. (1992). Synthetic aperture beamforming with automatic phase compensation for high frequency sonars, *Autonomous Underwater Vehicle Technology, 1992. AUV'92., Proceedings of the 1992 Symposium on*, IEEE, pp. 236–245.

Soumekh, M. (1994). *Fourier Array Imaging*, Prentice Hall, Englewood Cliffs, NJ, USA.

Synnes, S. A., Hansen, R. E. & Sæbø, T. O. (2009). Assessment of shallow water performance using interferometric sonar coherence, *Proceedings of Underwater Acoustic Measurements 2009*, Nafplion, Greece.

Urick, R. J. (1983). *Principles of Underwater Sound*, Mcgraw-Hill Book Company.

Van Trees, H. L. (2002). *Optimum Array Processing (Detection, Estimation, and Modulation Theory, Part IV)*, Wiley-Interscience.

Sonar Systems

Edited by Prof. Nikolai Kolev

The book is an edited collection of research articles covering the current state of sonar systems, the signal processing methods and their applications prepared by experts in the field. The first section is dedicated to the theory and applications of innovative synthetic aperture, interferometric, multistatic sonars and modeling and simulation. Special section in the book is dedicated to sonar signal processing methods covering: passive sonar array beamforming, direction of arrival estimation, signal detection and classification using DEMON and LOFAR principles, adaptive matched field signal processing. The image processing techniques include: image denoising, detection and classification of artificial mine like objects and application of hidden Markov model and artificial neural networks for signal classification. The biology applications include the analysis of biosonar capabilities and underwater sound influence on human hearing. The marine science applications include fish species target strength modeling, identification and discrimination from bottom scattering and pelagic biomass neural network estimation methods. Marine geology has place in the book with geomorphological parameters estimation from side scan sonar images. The book will be interesting not only for specialists in the area but also for readers as a guide in sonar systems principles of operation, signal processing methods and marine applications.

How to reference

In order to correctly reference this scholarly work, feel free to copy and paste the following:

Roy Edgar Hansen (2011). Introduction to Synthetic Aperture Sonar, Sonar Systems, Prof. Nikolai Kolev (Ed.), ISBN: 978-953-307-345-3, InTech, Available from: http://www.intechopen.com/books/sonar-systems/introduction-to-synthetic-aperture-sonar

INTECH
open science | open minds